

Short Communication

Preparation of $\text{Sm}_{0.5}\text{Sr}_{0.5}\text{Co}_{0.2}\text{Fe}_{0.8}\text{O}_{3-\delta}$ /MWCNT Composites and their electrocatalytic activities for ORR and OER

Yuwei Wang, Yongwang Jiang, Tao Cong, Liquan Fan*, Xinyu Su, Xingmei Liu, Weichao Zhang, Xijun Liu

College of Materials Science and Engineering, Heilongjiang Provincial Key Laboratory of Polymeric Composite Materials, Qiqihar University, No.42, Wenhua Street, Qiqihar 161006, PR China

*E-mail: Liquan_Fan@163.com

Received: 9 October 2021 / Accepted: 15 November 2021 / Published: 6 December 2021

In the perovskite/carbon composite electrocatalyst, the carbon phase acts as the conductive framework to support the perovskite phase and at the same time make the current distribution more uniform and improve the electrical contact between the perovskite phase and the electrode. Here, to improve the ORR/OER activity of perovskite, $\text{Sm}_{0.5}\text{Sr}_{0.5}\text{Co}_{0.2}\text{Fe}_{0.8}\text{O}_{3-\delta}$ (SSCF28) nanofibers prepared by electrospinning are mixed with multi-walled carbon nanotubes (MWCNT) to obtain SSCF28/MWCNT composite catalyst. For SSCF28/MWCNT with the optimal mass ratio, the OER Tafel slope of is 85.8 mV dec^{-1} , and the ORR Tafel slope is only 67.3 mV dec^{-1} . SSCF28/MWCNT (1:5) shows good bifunctional electrocatalytic performance.

Keywords: $\text{Sm}_{0.5}\text{Sr}_{0.5}\text{Co}_{0.2}\text{Fe}_{0.8}\text{O}_{3-\delta}$; Multi-walled carbon nanotube; OER/ORR; Electrocatalyst

1. INTRODUCTION

In recent years, due to the development and utilization of oil, natural gas, and other fossil energy, economic development has been greatly accelerated, but the damage to the environment is also severe. And with the over-exploitation of these non-renewable resources, they will eventually be depleted, so it is very important to develop novel clean energy. Among the numerous rechargeable energy conversion systems, metal-air battery with relatively high theoretical energy density has attracted extensive attention. Oxygen reduction reaction (ORR) and oxygen evolution reaction (OER) are two important reactions that affect the performance of metal-air batteries[1-3].

ABO₃ perovskite-type oxide $\text{Sm}_{0.5}\text{Sr}_{0.5}\text{CoO}_{3-\delta}$ (SSC) has recently attracted increasing attention in the field of OER/ORR electrocatalysis, because of their flexible crystal and electronic structures and

non-stoichiometric chemical properties. Velraj et al. [4] verified the possibility of SSC as bi-functional catalyst for metal-air batteries for the first time. SSC had similar ORR and OER catalytic activity with perovskite $\text{La}_{0.6}\text{Ca}_{0.4}\text{CoO}_3$ (LCC) and better stability than LCC. Bu et al. [5] synthesized SSC hollow nanofibers (SSC-HF) by coaxial electrospinning. SSC-HF was hybridized three-dimensional N-doped graphene (2DNG) to form SSC-HF-3DNG (SSC-HG) catalyst, which exhibited remarkable ORR/OER activity in 0.1 M KOH. The synergistic effect between SSC and 3DNG plays a key role in this stable bi-functional electrocatalyst. Zhang et al. [6] prepared Ag-SSC composite catalysts by mixing SSC and conductive silver gel (Ag) uniformly by ultrasonic method. Ag-SSC composite catalyst has better electrocatalytic performance than pure SSC and Ag and shows excellent stability, higher than that of commercial Pt/C. Lee et al. [7] regulated the oxygen vacancy of $\text{Sm}_{0.5}\text{Sr}_{0.5}\text{CoO}_{3-\delta}$ (SSC) oxide by controlling the annealing temperature. It was found that the electrocatalytic properties of OER and ORR of SSC were significantly enhanced with the increase of oxygen vacancy concentration. To further improve the electrocatalytic performance of SSC, it is a feasible method to improve the electrical conductivity of SSC materials. In this paper, $\text{Sm}_{0.5}\text{Sr}_{0.5}\text{Co}_{0.2}\text{Fe}_{0.8}\text{O}_{3-\delta}$ (SSCF28) nanofibers were prepared by electrospinning. SSCF28 nanofibers were mixed with multi-walled carbon nanotubes (MWCNT) to form SSCF28/MWCNT composite catalysts and the OER/ORR electrocatalytic properties of SSCF28/MWCNT were studied.

2. EXPERIMENTAL SECTION

2.1. Preparation of catalysts

$\text{Sm}_{0.5}\text{Sr}_{0.5}\text{Co}_{0.2}\text{Fe}_{0.8}\text{O}_{3-\delta}$ (SSCF28) nanofibers were synthesized by electrospinning. The appropriate amount of polyvinylpyrrolidone (PVP) was dissolved into N, N-dimethylformamide (DMF) under magnetic stirring at ambient temperature. And then stoichiometric amounts of samarium nitrate ($\text{Sm}(\text{NO}_3)_3 \cdot 6\text{H}_2\text{O}$), strontium nitrate ($\text{Sr}(\text{NO}_3)_2$), cobalt nitrate ($\text{Co}(\text{NO}_3)_2 \cdot 6\text{H}_2\text{O}$), and iron nitrate ($\text{Fe}(\text{NO}_3)_3 \cdot 9\text{H}_2\text{O}$) (the molar ratio was 0.5:0.5:0.2:0.8) were added to the above solution and mixed thoroughly. The homogeneous electrospinning solutions formed through overnight stirring. Four kinds of as-electrospinning precursor nanofibers were dried at 200 °C for 2 h in a vacuum drying chamber and then calcined in air at 800 °C for 2 h to obtain SSCF28 nanofibers.

The purchased commercial MWCNTs (from Shenzhen Nanport Co., LTD) were used as received. were oxidized to produce lots of electrochemically active sites on their surfaces [8]. MWCNTs were stirred in the mixed solution of H_2SO_4 (98 wt%) and HNO_3 (69 wt%), then ultrasonic treated for 2 h, and then washed to neutral with deionized water. The whole process was carried out in the ventilation cabinet. Finally, the washed MWCNTs were dried thoroughly. The prepared SSCF28 and MWCNTs were uniformly mixed by ultrasonic to prepare SSCF28/MWCNT composite catalysts with different mass ratios (1:1, 1:3, 1:5, 1:7).

2.2. Characterization and test

The microstructure of all the samples was examined by scanning electron microscopy (SEM, Hitachi S-4300) with the accelerating voltage of 10 kV. Transmission electron microscopy (TEM) was performed by H-7650 (Hitachi, Japan) at the accelerating voltage of 200 kV. X-ray diffraction (XRD) patterns were obtained by an D8 X-ray diffractometer assembled with a Cu K α radiation source.

The electrochemical impedance spectra (EIS) were characterized by the typical three-electrode system using the CHI 760E electrochemical workstation with a modulation amplitude of 5 mV and a frequency varying from 100 kHz to 0.1 Hz. For ORR/OER test, electrochemical tests were performed on a rotating ring disk electrode device (RRDE, ALS Co., Ltd.). GCE is used as the working electrode (diameter: 4mm), Ag/AgCl as the reference electrode, and platinum wire as the counter electrode. 0.1 M KOH solution was used as the electrolyte. Prior to electrochemical tests, oxygen was introduced into the electrolyte at least for 30 min. Linear sweep voltammetry (LSV) curves were examined at the rotating rate of 1600 rpm and the scan rate of 5 mV s⁻¹.

3. RESULTS AND DISCUSSION

The SEM image of the as-electrospun SSCF28 after calcination at 800 °C for 2 h is shown in Fig. 1(a).

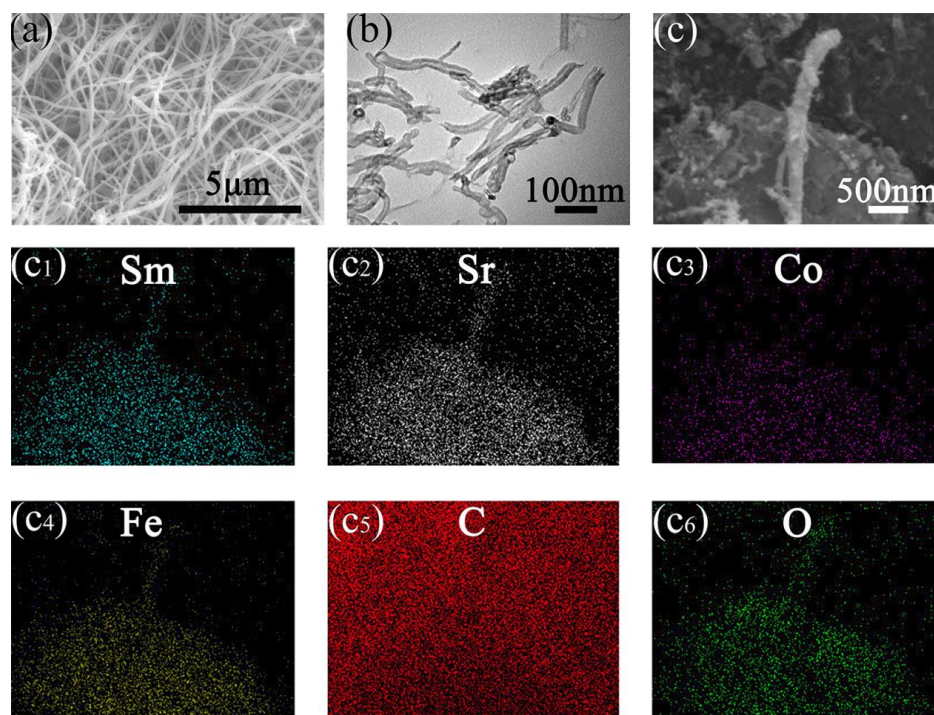


Figure 1. (a) SEM image of SSCF28. (b) TEM image of MWCNTs. (c) SEM image of SSCF28/MWCNTs. (c1)-(c6) EDS element mappings of Fig. 1(c).

The SSCF28 nanofibers have roughly a few hundred nanometers in diameter, and exhibits the formation of porous one-dimensional (1D) nanofibers, in agreement with the previous report [9]. A typical TEM image (Fig. 1(b)) indicates that the MWCNT after acidic etching and ultrasonic treatment were successfully shortened and showed good dispersion. Fig. 1(c) shows the SEM image of SSCF28/MWCNT. Fig. 1(c1-c6) is the EDS image of Fig. 1c, which clearly shows the uniform distribution of Sm, Sr, Co, Fe, C, and O elements. The clear implication of these results is that SSCF28 nanofibers are uniformly mixed with MWCNT for the SSCF28/MWCNT composite.

Fig. 2 presents XRD patterns for SSCF28, MWCNTs, and SSCF28/MWCNT composite in 1:5 mass ratio of SSCF28 to MWCNT (hereafter referred to simply as SSCF28/MWCNT (1:5)). The measured XRD patterns of SSCF28 and MWCNT are also given as guides to the eyes at the bottom of Fig. 2. SSCF28 is a kind of ABO_3 type perovskite oxides with high structure stability [10]. The XRD pattern of SSCF28/MWCNT shows broad amorphous features associated with MWCNT. The existence and distribution of MWCNT can also be proved by the EDS analysis of Fig. 1(c5). Apart from that, all the other diffraction peaks were indexed to SSCF28. Thus, we can say the perovskite/carbon composite catalysts were successfully prepared by ultrasonic mixing of SSCF28 and MWCNT.

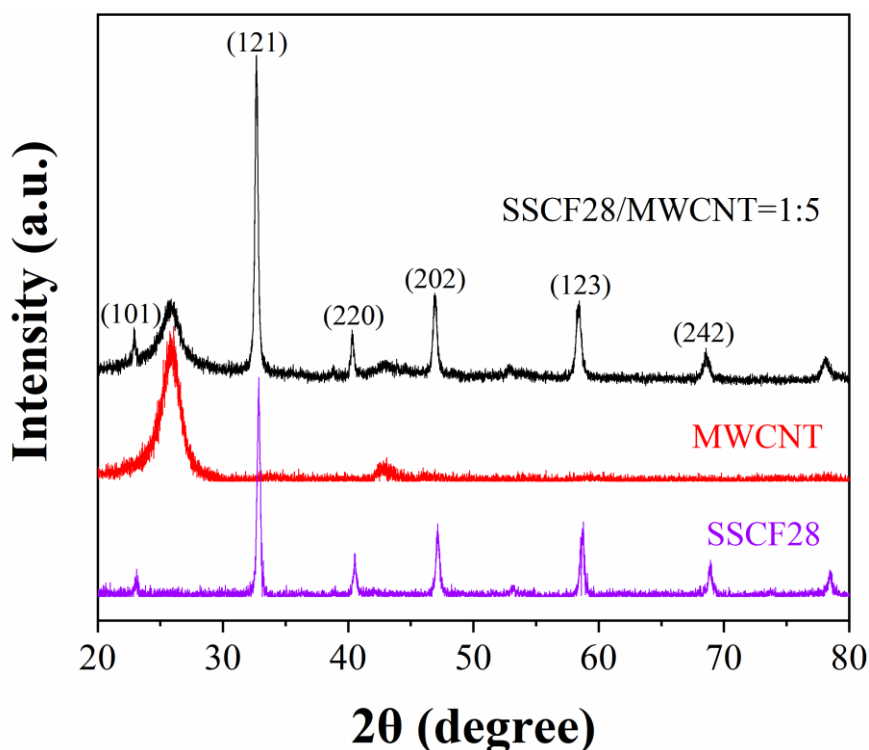


Figure 2. XRD patterns of pure SSCF28, pure MWCNT, and SSCF28/MWCNT composite (1:5 mass ratio).

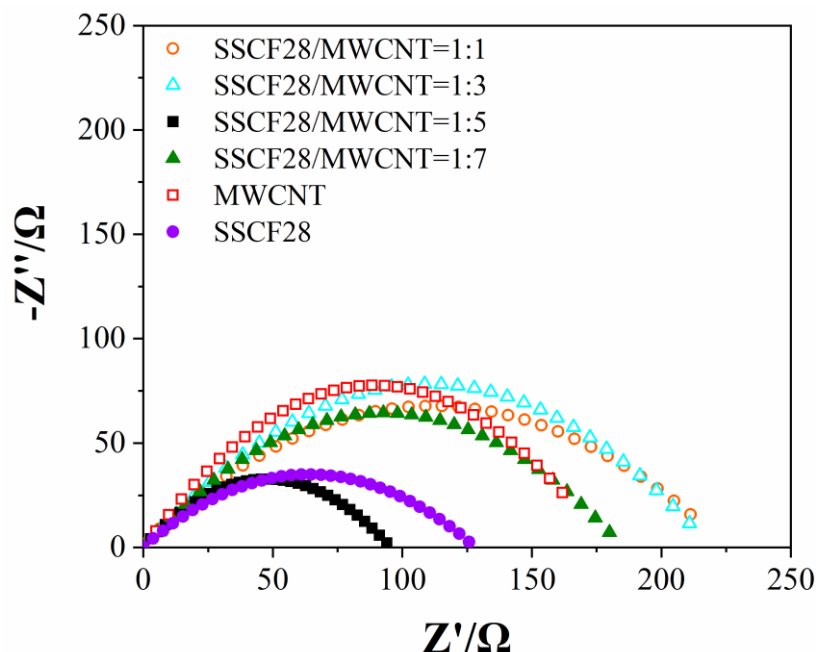


Figure 3. Nyquist plots for SSCF28/MWCNT recorded at 1.664 V (vs. RHE).

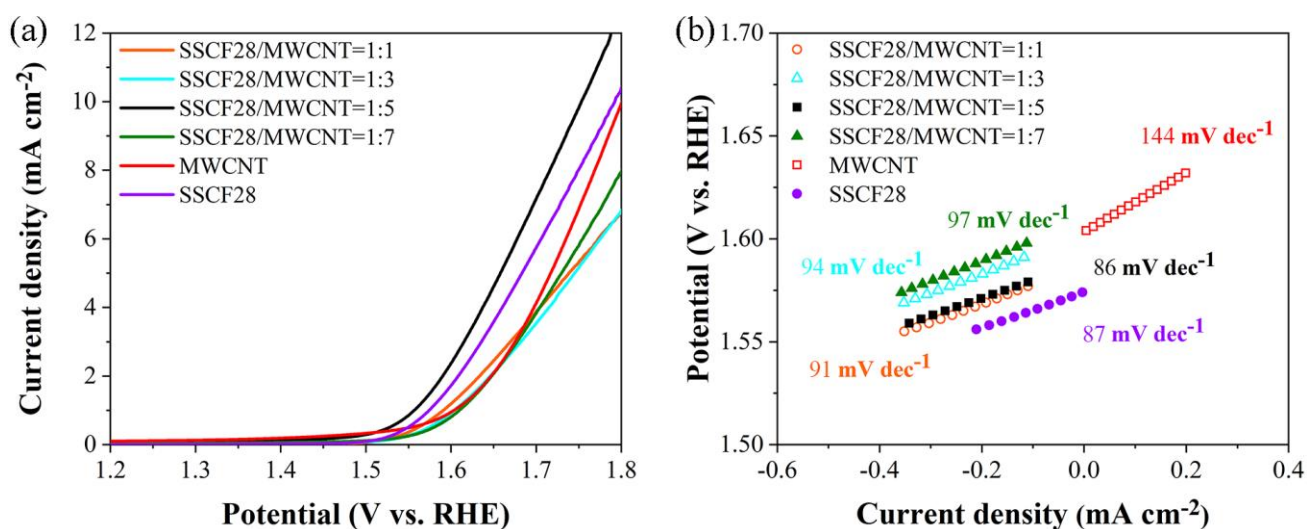


Figure 4. OER activity of SSCF28/MWCNT: (a) Polarization curve in 0.1 M KOH solution at a scan rate of 5 mV s^{-1} , (b) Tafel plots obtained from the polarization curves in OER process.

Fig. 3 shows the electrochemical impedance spectra (EIS) of SSCF28/MWCNT composite catalyst with the different mass ratios of SSCF28 to MWCNT at 1.664V. It can be seen that the resistance of SSCF28/MWCNT (1:5) is only 94Ω , which is smaller than that of SSCF28, MWCNT, and the other SSCF28/MWCNT composite catalysts. SSCF28/MWCNT (1:5) shows the lowest charge-transfer resistance. The EIS analysis reveals that the enhanced electron and charge transport capability at the SSCF28/MWCNT (1:5) electrode and the KOH electrolyte interface, which is favor for the ORR/OER catalytic kinetics [11]. The moderate introduction of MWCNT greatly improves the electronic conductivity of SSCF28 perovskite oxides. The SSCF28/MWCNT (1:5) catalyst with the optimal

electronic property and surface composition shows the lowest charge transfer resistance value and has the best electronic conductivity.

In order to explore whether the introduction of MWCNT can enhance the OER performance of SSCF28, the OER activity of SSCF28/MWCNT composite catalysts with different mass ratio was examined. Fig. 4(a) and (b) show the polarization curves and Tafel plots of the SSCF28/MWCNT composite catalysts, respectively. As shown in Fig. 4(a), the potential of SSCF28/MWCNT (1:5) is 1.753 V at 10 mA cm^{-2} , which is better than that of the single SSCF28, MWCNT and the other SSCF28/MWCNT composite catalysts. The Tafel slope of SSCF28/MWCNT (1:5) shows the lowest value of only 85.8 mV dec^{-1} , shown in Fig. 4(b). The SSCF28/MWCNT (1:5) exhibits the best catalytic performance for OER, which is in agreement with EIS analysis. After the treatment of ultrasound and mixed acid, the length of commercial MWCNTs were obviously shortened and showed good dispersibility. These factors are beneficial to the OER reaction. The SSCF28/MWCNT composite catalyst was prepared by ultrasonic method, which makes full contact between MWCNTs and SSCF28 perovskite nanofibers, leading to the improved electronic conduction pathways. The SSCF28/MWCNT composite with three-dimensional network-like porous structure can provide more electrocatalytic active sites and oxygen transport channels, resulting in better OER electrocatalytic performance.

Fig. 5(a) shows the ORR polarization curve of the SSCF28/MWCNT composite catalysts. The current density of SSCF28/MWCNT (1:5) is 3.88 mA cm^{-2} and the half-wave potential is 0.62 V at 0.2 V . Fig. 5(b) shows the Tafel plots of the SSCF28/MWCNT composite catalyst. SSCF28/MWCNT (1:5) has the lowest Tafel slope of 67.3 mV dec^{-1} . SSCF28/MWCNT (1:5) shows the best ORR performance. To evaluate the bifunctional electrocatalytic performance, the potential gap ($\Delta E = E_{j10, \text{OER}} - E_{1/2, \text{ORR}}$) for SSCF28/MWCNT (1:5) was calculated as shown in Table 1 below. For the sake of comparison, the ΔE values of some perovskite catalysts reported in literature are also summarized in Table 1. The ΔE value of SSCF28/MWCNT (1:5) was calculated to be 1.13 V , which is close to comparable reported values[12-15].

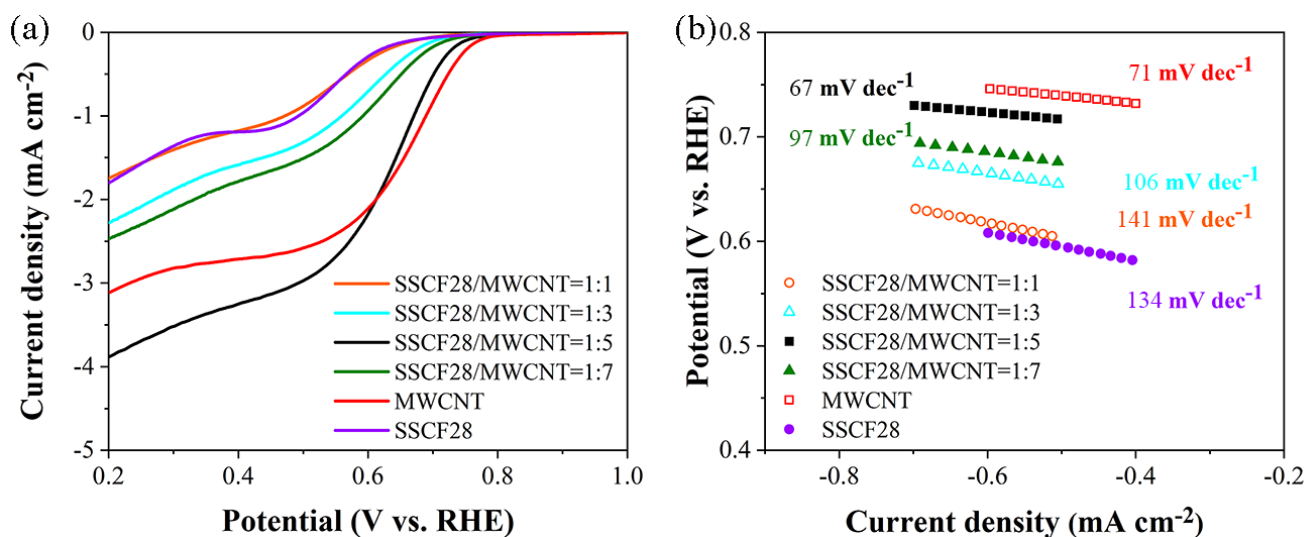


Figure 5. ORR activity of SSCF28/MWCNT: (a) Polarization curve in O₂ saturated 0.1 M KOH solution at a scan rate of 5 mV s^{-1} , (b) Tafel plots derived from the LSV curves.

Table 1. The potential gap (ΔE) values of reported perovskite/carbon catalysts in literature

Perovskite/carbon catalysts	ΔE	References
SSCF28/MWCNT	1.13	Our work
LaNi _{0.85} Mg _{0.15} O ₃ /VC	1.21	[12]
La _{0.6} Sr _{0.4} CoO _{3-δ} /VC	1.15	[13]
Pr _{0.5} Ba _{0.5} MnCo _{0.2} O _{3-δ} /VC	1.13	[14]
BaMnO ₃ /C	1.25	[15]

4. CONCLUSIONS

SSCF28/MWCNT composite catalysts were prepared by using ultrasonic method. The introduction of MWCNT after acidizing greatly improves the electronic conductivity of SSCF28 with three-dimensional network structure. The moderate amount of MWCNT provided a lot of active sites and oxygen transport channels for electrocatalytic reaction of the catalysts. SSCF28/MWCNT with the mass ratio of 1:5 showed the best electrocatalytic performance. The potential gap of SSCF28/MWCNT(1:5) was 1.133 V, close to some comparable perovskite/carbon composite catalysts. SSCF28/MWCNT(1:5) had good OER/ORR activities.

ACKNOWLEDGMENTS

The Natural Science Foundation of Heilongjiang Province, China (No. LH2019E092), and the Fundamental Research Funds in Heilongjiang Provincial Universities (No. 135309347).

References

1. W. Sun, F. Wang, B. Zhang, M. Zhang, V. Küpers, X. Ji, C. Theile, P. Bieker, K. Xu, C. Wang and M. Winter, *Science*, 371 (2021) 46–51.
2. C. Liu, P. Zuo, Y. Jin, X. Zong, D. Li, Y. Xiong, *J. Power Sources*, 473 (2020) 228604.
3. C. Liu, Z. Wang, X. Zong, Y. Jin, D. Li, Y. Xiong, G. Wu, *Nanoscale*, 12 (2020) 9581-9589.
4. S. Velraj, J.H. Zhu, *J. Power Sources*, 227 (2013) 48–52.
5. Y. Bu, G. Nam, S. Kim, K. Choi, Q. Zhong, J.H. Lee, Y. Qin, J. Cho, G. Kim, *Small*, 14 (2018) 1802767
6. Y. Zhang, Y. Guo, T. Liu, F. Feng, C. Wang, H. Hu, M. Wu, M. Ni, Z. Shao, *Front. Chem.*, 7 (2019) 524.
7. H. Lee, O. Gwon, K. Choi, L. Zhang, J. Zhou, J. Park, J.W. Yoo, J.Q. Wang, J.H. Lee, G. Kim, *ACS Catal.*, 10 (2020) 4664–4670.
8. C. Yang, X. Hu, D. Wang, C. Dai, L. Zhang, H. Jin, S. Agathopoulos, *J. Power Sources*, 160 (2006) 187-193.
9. L. Fan, T. Cong, X. Su, Y. Wang, X. Liu, W. Zhang, Y. Li, D. Zhang, *Int. J. Electrochem. Sci.*, 16 (2021) A.
10. P. Anand, M. Wong, and Y. Fu, *Sustainable Energy Fuels*, 5 (2021) 4858.
11. C. Liu, Z. Wang, X. Zong, Y. Jin, D. Li, Y. Xiong, and G. Wu, *Nanoscale*, 12 (2020) 9581-9589.

12. Z. Du, P. Yang, L. Wang, Y. Lu, J. B. Goodenough, J. Zhang, D. Zhang, *J. Power Sources*, 265 (2014) 91.
13. M. Y. Oh, J. S. Jeon, J. J. Lee, P. Kim, K. S. Nahm, *RSC Adv.*, 5 (2015) 19190.
14. Y. Zhang, Y. Sun, J. Luo, *ECS Trans.*, 75 (2016) 955.
15. Y. Xu, A. Tsou, Y. Fu, J. Wang, J.-H. Tian, R. Yang, *Electrochim. Acta*, 174 (2015) 551.

© 2022 The Authors. Published by ESG (www.electrochemsci.org). This article is an open access article distributed under the terms and conditions of the Creative Commons Attribution license (<http://creativecommons.org/licenses/by/4.0/>).